



# Fault zone geology: lessons from drilling through the Nojima and Chelungpu faults

Anne-Marie Boullier

## ► To cite this version:

Anne-Marie Boullier. Fault zone geology: lessons from drilling through the Nojima and Chelungpu faults. 2011. insu-00590704

**HAL Id: insu-00590704**

**<https://hal-insu.archives-ouvertes.fr/insu-00590704>**

Preprint submitted on 4 May 2011

**HAL** is a multi-disciplinary open access archive for the deposit and dissemination of scientific research documents, whether they are published or not. The documents may come from teaching and research institutions in France or abroad, or from public or private research centers.

L'archive ouverte pluridisciplinaire **HAL**, est destinée au dépôt et à la diffusion de documents scientifiques de niveau recherche, publiés ou non, émanant des établissements d'enseignement et de recherche français ou étrangers, des laboratoires publics ou privés.

# **Fault zone geology: lessons from drilling through the Nojima and Chelungpu faults**

Anne-Marie Boullier

ISTerre - CNRS, Université Joseph Fourier, Maison des Géosciences, BP 53, 38041  
GRENOBLE CEDEX 09, France

e-mail: Anne-Marie.Boullier@obs.ujf-grenoble.fr

## **Abstract**

Several drilling projects have been conducted through active faults with the aim of learning about the geology of the fault zones and tentatively correlating the structure and mineralogy of the fault zones with their seismological behaviour during recent earthquakes. Here we present the major results obtained from structural and mineralogical studies of core samples retrieved from the dextral reverse strike-slip Nojima Fault (Japan) within granitic rocks following the Kobe earthquake (1995), and from the Chelungpu thrust Fault (Taiwan) within alternating silts and shales following the Chi-Chi earthquake (1999). We show how these projects, despite not fulfilling all their objectives, have still contributed to a better geological knowledge of the fault zones, to a better characterization of the slip zones related to the recent earthquakes particularly of their thickness, microstructures and deformation mechanisms, and to a better understanding of the nature and role of fluids within the fault zone. They also have led to new questions, and to new approaches for studying fault rock samples. For all these reasons, they have stimulated international scientific research about fault zone geology.

13098 words, 117 references, 1 table, 6 figures

Abbreviated title: Fault zone geology



In 1993, a conference was held in California on Mechanical Effects of Fluids in Faulting. This led to a special issue of the Journal of Geophysical Research in the introduction of which Hickman *et al.* (1995) reported recommendations about three significant topics for future research, one of which was "fault zone drilling combined with surface-based geophysical and geological investigations". Since that time, several fault-zone drilling projects have been conducted around the world, such as the Nojima Fault project following the 1995 Kobe Earthquake, the Corinth Rift (Greece) Laboratory, the San Andreas Fault Observatory at Depth (SAFOD) in Parkfield (California), the Taiwan Chelungpu fault Drilling Project (TCDP) following the 1999 Chi-Chi Earthquake and the Wenchuan earthquake Fault Scientific Drilling (WFSD) through the Longmen Shan active fault zone (following the 2008 Wenchuan earthquake, China). Other projects have drilled plate boundaries along subduction zones, such as the shallow Barbados accretionary prism (Leg ODP 156) or the NanTroSeize experiment which is still in progress through the Nankai Trough.

In a recent review, Zoback *et al.* (2007) summarize the principal objectives and scientific goals of fault-zone drilling: "The objective of fault-zone drilling projects is to directly study the physical and chemical processes that control deformation and earthquake generation within active fault zones." More recently, the ICDP-SCEC international workshop on "Rapid Response Drilling: Past, Present, and Future", held in Tokyo, Japan (November 2008, see Brodsky *et al.* 2009), pointed out the need to know how fault strength recovers slowly in the long interval between earthquakes and what combinations of physical and chemical properties of fault rocks lead faults to slip or to creep. In order to fulfill these objectives, the active fault zone and active slip zone related to the last earthquake had to be first recognized so their thickness, mineralogy, chemical composition, and microstructures could be studied. The major geological questions addressed by fault zone drilling projects are the following: can we interpret microstructures in terms of deformation mechanisms, strain-rate, slip-weakening or hardening processes? Can we estimate the fracture and heat contribution in the energy budget of an earthquake? What is the importance of fluids before, during and after an earthquake? What are the mechanisms and kinetics of fault healing? What are the physical properties (seismic velocities, electrical resistivity, density, porosity, permeability) of fault-zone materials compared to country rocks and how do they vary in time and space? As predicted by Hickman *et al.* (1995), these drilling programs have

partly answered these questions and contributed to a better knowledge of the active faults, as illustrated by the huge number of scientific papers that have arisen from the studies of core samples; in fact these are too numerous to cite herein. These studies have also led to definition of important new questions and have stimulated a large number of laboratory measurements and experiments.

Of course, boreholes are needle points through faults and surface surveys and detailed studies should not be neglected. However, they provide continuous and unaltered sampling through the faults. In this paper, I will focuss on and tentatively summarize the main results that have specifically arisen from the Nojima (Japan) and Chelungpu (Taiwan) drilling projects.

## **The Nojima Fault (Japan)**

### ***General context***

The 1995 Hyogo-ken Nanbu earthquake (Kobe earthquake, M7.2) caused 6432 fatalities and disastrous damage in the Kobe city and Awaji Island area. One year after the earthquake, five boreholes were successfully drilled through the Nojima Fault in Awaji Island by the Geological Survey of Japan (GSJ) and the National Research Institute for Earth Science and Disaster Prevention (NIED) at Hirabayashi, and by the Disaster Prevention Research Institute (DPRI, Kyoto University) at Ogura, with the aim of better understanding seismic processes. These boreholes, which were completed within 14 months of the Kobe earthquake, were the first to penetrate through active faults following a recent earthquake. The Nojima Fault is a north-east striking and south-east dipping dextral reverse fault running along the west coast of the Awaji Island, which cuts across the Cretaceous Ryoke granodiorite and its porphyry dykes (Figure 1a). Its Quaternary offset and average slip rate have been established by Murata *et al.* (2001) to be 490-540m and 0.4-0.45m/10<sup>3</sup> years, respectively, for the last 1.2 my based on the displacement of an unconformity below the sedimentary Kobe Group (Figure 1b). The basal part of this group has been dated to Middle to Late Eocene (Yamamoto *et al.* 2000), i.e. 40 Ma. These geological data and dates represent important constraints for

interpreting the structure and mineralogy of the fault rocks observed in core samples.

### ***The active fault zone***

Drill holes were nearly vertical and at low angle to the orientation that is inferred for the Nojima Fault from its steeply dipping surface rupture (75° to 85° southeast, Awata & Mizuno 1998). Conventional borehole logging during drilling illustrated the evolution of physical properties of rocks with depth. Measured parameters were sonic wave velocity (Vp), borehole diameter, resistivity, porosity, density, gamma ray, temperature (Ito *et al.* 1996; Ikeda 2001). By combining these data with continuous observation of core samples on-site, the main fault zone was able to be located at 389.5m, 624.5m and 1140m depth in the DPRI 500, Hirabayashi GSJ and NIED drill holes, respectively (Figure 1b and c). Another borehole approached the fault at ca. 1700m depth (DPRI 1800, Figure 1b) but did not go entirely through it (Lin *et al.* 2007).

The logging tools give a first image of the structure of the fault. In the GSJ borehole for example, the resistivity decreases regularly above and increases abruptly below all faults regardless of their importance (Pezard *et al.* 2000). Conversely, the natural gamma radioactivity displays a wide maximum above the fault, decreases sharply on the fault and then increases regularly below it, until the base-line (Pezard *et al.* 2000). Both trends indicate an asymmetry of the fault zone and a tendency towards more extensive fracturing and alteration of the hanging-wall as the fault is approached. This result illustrates that logging tools are powerful methods to locate damage and fault zones in boreholes. The Stoneley wave analysis was used to determine the location of the permeable zone around the Principal Slip Zone (PSZ, Sibson 2003) in the Hirabayashi GSJ drill hole within the 623 to 625m depth interval predicted by observations of the surface rupture (Kiguchi *et al.* 2001). It is important to note that no temperature anomaly was measured in any borehole.

### ***Characterization of the fault zone***

An identical procedure was followed for core handling for all drill holes (Tanaka *et al.*

2001 a; Matsuda *et al.* 2001; Lin *et al.* 2007). Core pieces were fixed using epoxy resin and cut in two halves. One of these halves was for archiving, but was polished for naked-eye observations. The other half was made into thin sections, and used for experiments and analyses. This method presented advantages for microstructural studies because it allowed multiscale observations of samples from cores to thin sections. However, it caused complications in the measurement of physical properties of the fault rocks.

Formation Micro-Imaging (FMI™; Schlumberger, Houston, Texas), a downhole logging technique which was performed after the GSJ drilling, provides an image of the electric resistivity of the borehole and thus indicates the number and orientation of the fractures. The fractures tend to strike E-W far from the fault, as expected due to the orientation of the present-day stress field, but they become normal to the fault close to it and parallel to it within the fault core (Ito & Kiguchi 2005). FMI and images of the core were compared to reorient the core samples in a geographic coordinate system (Ohtani *et al.* 2000 a). However, this was not possible for the whole length of the borehole, particularly in sections with few fractures. Nevertheless, observations of thin sections normal to the core indicate evidence for two nearly orthogonal directions of compression in the form of kinked biotites (Boullier *et al.* 2004 a), healed (fluid inclusion planes) or sealed (calcite) microfractures (Takeshita & Yagi 2001). These two stress tensors are consistent with the geodynamics of Japan which displays left-lateral transcurrent faults striking 045° during the Late Cretaceous-Palaeocene (Kanaori 1990), which were reactivated as right-lateral faults during Late Pliocene to Quaternary times (Fabbri *et al.* 2004).

Systematic studies of polished slabs (see for example Figure 2) and thin sections have provided important data on the distribution of deformation microstructures, geochemical composition and mineralogy of the core samples in all boreholes (Ohtani *et al.* 2000 b, 2001; Fujimoto *et al.* 2001; Tanaka *et al.* 2001 a, b, 2007 a; Kobayashi *et al.* 2001; Matsuda *et al.* 2001, 2004; Lin *et al.* 2001, 2007). Most of these studies have used Sibson's (1977) classification of fault rocks. First, these authors have used distribution of deformation and alteration textures in order to define the fault core where most of the displacement is accommodated, and the damage zone that is made of a network of subsidiary structures between the fault core and the undeformed protolith (Caine *et al.* 1996). The fault core and damage zone are 0.3m and > 46.5m wide, respectively, in the Hirabayashi GSJ borehole (Ohtani *et al.* 2000 b, 2001; Fujimoto *et al.* 2001; Tanaka *et al.*

2001 *a*). The fault damage zone is 70m wide in the Hirabayashi NIED drill hole (Tanaka *et al.* 2007 *a*) and even larger (130m) if the 1140m and 1312m fault zones are considered as bounding faults of a fault zone (Lockner *et al.* 2009). The Nojima fault zone becomes wider and more complex with depth, branching into two faults between the Hirabayashi GSJ and NIED drill holes.

Secondly, correlations between deformation intensity and geochemical composition were possible thanks to the homogeneity of the starting material, the Ryoke granodiorite (Figure 2a). Mass balance calculations considering  $\text{TiO}_2$  and  $\text{P}_2\text{O}_5$  as immobile elements indicate important volume loss (compaction) in the fault core but volume gain (dilation) in the damage zone in the Hirabayashi GSJ and NIED boreholes (Tanaka *et al.* 2001 *a*, 2007 *a*). Volume gain in the damage zone corresponds also to an LOI (Losses On Ignition) increase and to decrease of the P-wave velocity (Fujimoto *et al.* 2001). These results are consistent with permeability and strength evolution around the fault as measured by Mizoguchi *et al.* (2008 *a*) on surface samples and by Lockner *et al.* (2009) on drill core samples. The fault zone is "a thin, low-strength, low-permeability fault zone core flanked by zones of high permeability rock that have undergone relatively limited total shear" (Lockner *et al.* 2009).

### ***The Principal Slip Zone***

Although it was a challenging prospect, the Principal Slip Zone (PSZ, Sibson 2003), where displacement took place during the Kobe earthquake, was located by careful observations of core samples and polished slabs from three drill holes. In the DPRI 500 drill hole (Figure 1b) the PSZ is localized at the contact between foliated goudes from the Ryoke granodiorite and from the Osaka group, and is described as a fault surface (Lin *et al.* 2001; Tanaka *et al.* 2001 *b*). This would suggest that PSZ related to the Kobe earthquake has no apparent thickness at this depth. However, thanks to electron spin resonance (ESR) intensity measured across the dark gray fault plane by Fukuchi & Imai (2001), and to comparison of ESR analyses of natural and experimental fault gouge samples produced from high-speed slip tests (Fukuchi *et al.* 2005), it has been demonstrated that a thermal effect related to the earthquake was recorded in a 6mm wide zone, which could be explained by frictional heating of the pore water in the fault

gouge above boiling, and its diffusion into the fault gouge (Fukuchi & Imai 2001). Darkening of the gouge and the presence of an increased ferrimagnetic resonance (FMR) signal in the PSZ are related to the formation of ferri-magnetic iron oxides and indicate that frictional heating may have induced temperatures of at least 350-400°C during seismic slip at 390m depth (Fukuchi *et al.* 2005).

In the Hirabayashi GSJ drill hole (Figure 1c), after much debate it was concluded that the PSZ was found at 625.27m depth in a millimetre-thick slip zone (Tanaka *et al.* 2001 *a*). In the Hirabayashi NIED drill hole (Figure 1c), Tanaka *et al.* (2007 *a*) located the PSZ at 1140.57 to 1140.66m depth in a 10 mm-thick Ca-rich ultracataclasite layer in which intense grain-size reduction has occurred, but Lockner *et al.* (2009) suggested that two activated fault strands were crossed by this drill hole at 1140 and 1312m depth. All these observations on drill holes through the Nojima fault demonstrate that thickness of the PSZ increases with depth and that fault healing processes may be very efficient, making it difficult to recognize the PSZ in all drill holes only one year after the Kobe earthquake.

### ***Pseudotachylytes and seismic processes***

The most striking rocks observed either in GSJ or NIED drill holes are pseudotachylytes (Figures 2c and 3a) which are associated with ultracataclasites (Ohtani *et al.* 2000 *b*; Tanaka *et al.* 2001 *a*; Boullier *et al.* 2001; Otsuki *et al.* 2003). These rocks are rarely observed in faults as predicted by Sibson & Toy (2006), but clearly result from seismic slip (Sibson 1975) and therefore provide information on seismic processes and the energy budget of earthquakes (Kanamori & Heaton, 2000). Otsuki *et al.* (2003) suggested that the ultracataclasites observed in these drill holes behaved as fluidized granular material, in which frictional resistance decreased abruptly to nearly zero during seismic slip. They also proposed that the viscosity of the pseudotachylytic melt evolved during seismic slip, based on the temperature reached and the percentage of unmelted grains. As observed in the Hirabayashi GSJ drill hole and surface outcrops, the pseudotachylytes are laminated with some contorted and folded layers (Figure 3a; Tanaka *et al.* 2001 *a*; Boullier *et al.* 2001; Otsuki *et al.* 2003) that could be indicators of high-velocity seismic slip (Mizoguchi *et al.* 2009). The glass is not recrystallized and

does not display spherulites or crystallites as often described in pseudotachylytes (see for example di Toro & Pennachioni 2004). However, there are abundant rounded vesicles which appear to be fluid inclusions (Figure 3b). Microthermometry on some of these fluid inclusions indicates that they are filled by a very dense CO<sub>2</sub>-H<sub>2</sub>O fluid. The intersection of isochoric lines with the present-day 24°C/km geothermal gradient indicates that the fluid inclusions were trapped at 380°C and 410MPa (Boullier *et al.* 2001) or at 270°C and 250MPa if a 30°C/km geothermal gradient is considered (Boullier *et al.* 2004 *a*). The lower estimate is probably more realistic as no mylonites were found in the Nojima fault. Such trapping conditions imply that these pseudotachylytes were formed at >9km depth in the seismogenic zone before exhumation of the Ryoke granodiorite and deposition of the Kobe group at 40Ma. They therefore formed during an early stage of seismic activity on the Nojima Fault (Boullier *et al.* 2001). This deduction has been confirmed by fission track data of zircon which provided a 56 Ma age for the pseudotachylytes (Murakami & Tagami 2004). The presence of fluid inclusions also indicates that the pseudotachylytic melt was saturated in fluids when cooling which suggests that this frictional melt formed in an already altered initial material containing fluid as a free phase or/and structurally bound in minerals. Famin *et al.* (2008) measured the CO<sub>2</sub> and H<sub>2</sub>O contents of the pseudotachylytic melts by Fourier transform infrared (FTIR) microanalysis, illustrating that the younger layers have decreasing CO<sub>2</sub> contents due to decreasing pressure of formation and that a significant mass of CO<sub>2</sub> may be exsolved during each pseudotachylyte-generating seismic event. Consequently, because CO<sub>2</sub> saturation in silicate melts is pressure-dependent, CO<sub>2</sub> content in pseudotachylytic glass may be used as a proxy for the depth of pseudotachylyte formation.

### ***Energy budget of the earthquake***

Boullier *et al.* (2001) used the calculations proposed by Kanamori & Heaton (2000) to evaluate the thermal budget of earthquakes that resulted in pseudotachylyte formation. Based on the thickness of the pseudotachylyte layers (1mm) and on the temperature increase due to frictional melting (1000°C), they deduced that each pseudotachylyte layer corresponds to M6 to M7 earthquakes assuming a 3-4MPa initial frictional stress

calculated by Bouchon *et al.* (1998) from the slip model of Irikura *et al.* (1996). Therefore, the pseudotachylytes observed now at 625m depth in the Hirabayashi GSJ borehole were formed during *ca.* 56Ma old earthquakes similar in magnitude (M6 to M7 versus Mw 6.9) to the recent Kobe earthquake.

Grain-size distribution (GSD) has been recently used by many authors to characterize fault rocks and gouges related to seismic events, with the aim of estimating the fracture energy of earthquakes (see a review in Keulen *et al.* 2007). This technique has also been used to characterize aseismic faulting and cataclasis accompanying hydrothermal alteration in a the Cajon Pass drill hole (Blenkinsop & Sibson 1992). Keulen *et al.* (2007) measured GSD in cataclasites from the Hirabayashi GSJ drill hole and in experimentally deformed granitoids. In both cases GSD were not fractal and two slopes (D) were observed in all log-log GSDs. In experimental or natural examples, D-values of 0.9-1.1 were measured for grains smaller than *ca.* 1  $\mu\text{m}$ . Two different D were measured for cracked grains (1.5-1.6) and gouges (2.0 to 2.6) for grains larger than 1  $\mu\text{m}$ , which is the grinding limit of quartz. These results show that grain size reduction in fault zones develops by a two-stage process: rupturing creates cracked grains; further displacement of fragments causes further comminution by wear and attrition. Healing processes may also modify GSD as demonstrated by experiments of hydrostatic or non-hydrostatic healing of fault gouges (Keulen *et al.* 2008). Thus, we should be cautious when using GSD for calculating the fracture energy of an earthquake because GSD is the sum of several cumulated seismic events and is the product of different mechanisms occurring during the whole evolution of the gouge zone.

### ***Fluids: before, during and after earthquakes***

Multi-stage alteration of fault rocks has been recognized by Ohtani *et al.* (2000 *b*), Fujimoto *et al.* (2001), Tanaka *et al.* (2001 *a*, 2007 *a*) and Boullier *et al.* (2004 *a*), as summarized in Table 1. Using the relationships between hydrothermal minerals and structures, it is possible to correlate hydrothermal alteration with deformation episodes. The older hydrothermal stage is weak, static and characterized by chlorite. It is attributed to the cooling of the granodiorite between 90 and 74 Ma (Takahashi 1992;



Murakami *et al.* 2002).

The second stage is widespread and, at least in the Hirabayashi GSJ drill hole, is represented by zeolites. Laumontite, the most common mineral formed in this stage, is observed throughout the damage zone as an alteration product of plagioclase, filling veins and sealing fractures. The hydrothermal alteration in the low-strain damage zone in the Hirabayashi GSJ drill hole is very similar to that observed in the Cajon Pass drill hole (Blenkinsop & Sibson, 1992) in terms of starting material (granitic rock), alteration product (laumontite formed at the expense of plagioclase) and deformation textures (almost no crack-seal textures, extensional fractures with flow structures and dilatant cataclasis). Some dilatant microstructures could thus result from aseismic deformation related to volume change induced by replacement of plagioclase by laumontite (Blenkinsop & Sibson, 1992). Laumontite is present as clasts in ultracataclasites (pale green in Figure 2b); in particular in those associated with pseudotachylytes. This indicates that the first stage of seismic activity and alteration occurred before 40Ma under decreasing pressure and temperature conditions between the formation of pseudotachylytes at  $>270^{\circ}\text{C}$  and  $>250\text{MPa}$  (see above), and the stability field of laumontite, which is between  $280^{\circ}\text{C}$  and  $150^{\circ}\text{C}$  depending on the pressure (Zen & Thompson 1974). These observations are also consistent with the decreasing  $\text{CO}_2$  content of the pseudotachylytic glass measured by Famin *et al.* (2008).

The third stage of alteration is characterized by thin veinlets of siderite emplaced within the flattening plane in cataclasites and ultracataclasites (reddish brown zones in Figure 2b) within the core of the main fault zone around 625m in the Hirabayashi GSJ drill hole (Boullier *et al.* 2004 *a*) and within the 1140m, 1300m and 1800m fault cores of the Hirabayashi NIED drill hole (Boullier, unpublished observations). These veins are not associated with any significant phase of deformation, nor with structures resulting from dilatancy and are deformed in later gouge zones or cross-cut by later carbonate veins (see Table 1 and Boullier *et al.* 2004 *a*). For these reasons they have been correlated with a quiescence stage by Boullier *et al.* (2004 *a*).

The fourth hydrothermal stage is characterized by hydraulic fractures filled by small grain-size euhedral ankerite and siderite crystals (pale honey-coloured fractures in Figure 2b; Fujimoto *et al.* 2001; Boullier *et al.* 2004 *b*; Moore *et al.* 2009). Undeformed hydrofractures of this type are mainly localized in the hanging-wall of the main fault

zone in the Hirabayashi GSJ drill hole but they are also observed below the fault where they are deformed by late gouge zones (Figure 3c). Their internal structure strongly suggests that they were induced by coseismic hydraulic fracturing and fast nucleation of carbonates due to a sudden fluid or CO<sub>2</sub> partial pressure drop due to fracturing (Boullier *et al.* 2004 *b*).

The latest stage of alteration is characterized by clays. Smectite has been found in the GSJ 625m (Fujimoto *et al.* 2001) and NIED 1140m (Matsuda *et al.* 2004) fault zones. Illite is also observed in small conjugate low-angle reverse shear zones located below the principal 625m fault core (Figure 3c) in which it displays a C/S microstructure (Figure 3d). These small shear zones lie below the principal 625m fault core and may be observed on the FMI images (Ito & Kiguchi 2005). They also correspond to the 625-635m depth interval where deformation of the borehole has been seen on the BHTV (BoreHole TeleViewer) acoustic scans (C  l  rier *et al.* 2000).

The present-day fluids which are circulating in the GSJ 625m fault zone have been analyzed. Their chemical composition is in equilibrium with the carbonates precipitated in the hydraulic fractures described above and with illite and Ca-montmorillonite. This also indicates that the fluids are flowing upwards and originate from a reservoir situated at 4km depth (Fujimoto *et al.* 2007) based on the 24  C geothermal gradient measured in the Hirabayashi GSJ borehole (Kitajima *et al.* 1998). Lin *et al.* (2003) have proposed that, because these fluids are meteoric in origin, they have infiltrated the active Nojima Fault by a fluid suction-pumping process inspired by the so-called seismic pumping model (Sibson *et al.* 1975).

### ***Processes of healing by dissolution-precipitation***

Fluids are also involved in the chemical compaction of gouges, ultracataclasites or fine-grained vein-filling material by dissolution-precipitation processes, although fluid advection is not necessary. Evidence for these processes has been found in the 625m fault zone of the Hirabayashi GSJ borehole in the form of stylolitic surfaces in fine-grained laumontite dilatant veins of the second hydrothermal stage (Boullier *et al.* 2004 *a*) and indentation of grains in gouges or in fine-grained carbonate veins of the third hydrothermal stage (Boullier *et al.* 2004 *b*). The dissolution-precipitation processes are

diffusion controlled, and therefore dependent on the diffusion distance between the source and sink of solute, and on the mineral which is dissolved (Gratier *et al.* 2003). Consequently, although these are very slow processes, they may be very efficient under low stresses in fine-grained material such as those mentioned above and therefore contribute to the post-seismic or interseismic sealing of the fault, to the decrease in permeability of very fine-grained ultracataclasites as measured by Lockner *et al.* (2009) and to stress build up in the lead-up to the next seismic rupture. Minerals involved in these processes are mostly laumontite during the first and carbonates during the second stages of seismic activity of the Nojima Fault. Decrease in permeability should result in an increase in fluid pressure. However, there are no observational data, such as horizontal extensional veins, that would suggest that an abnormal fluid pressure regime existed in the case of the Nojima Fault as for the fault-valve model (Sibson *et al.* 1988; Sibson 1990).

### ***Lessons from the Nojima Fault drilling projects.***

The first lesson from the Nojima Fault drilling projects is that geology of this fault is considerably more complex than initially thought. The fault-zone thickness, structure and mineralogy are the result of two distinct periods of seismic activity accompanied by intense hydrothermal alteration separated by a period of quiescence. All these stages are recorded in the fault rock microstructures. The recognition of very peculiar pseudotachylytes in the core of the fault that are attributed to the first period of activity has induced significant interest in this type of rocks. As a result, a number of high velocity rotary shear friction experiments have been performed on « hard » rocks (for example Hirose & Shimamoto 2005; Di Toro *et al.* 2004). Natural gouges from the Nojima Fault have also been used as initial material for similar high velocity experiments to investigate their behaviour during seismic slip (Mizoguchi *et al.* 2009). Observations of the internal structure of the Nojima Fault have also illustrated that we need more information on the permeability and thermal properties of faults to understand and predict their seismological behaviour (for example Wibberley & Shimamoto 2003, 2005; Uehara & Shimamoto 2004; Mizoguchi *et al.* 2008 *a*; Lockner *et al.* 2009). Permeability is highly dependent on fracturing and healing processes, and

rates and kinetics of these processes are of considerable importance. Recently, highly permeable pulverized rocks have been discovered along the San Andreas Fault by Dor *et al.* (2006) and along the Arima-Takatsuki tectonic line (Mitchell *et al.* 2009). Some textures of dilatant fractures at depth in the Hirabayashi GSJ drill hole are similar to naturally (Rockwell *et al.* 2009) and experimentally (Doan & Gary 2009) pulverized samples. Could they be the expression of pulverization at depth or high strain-rate brittle deformation in the fault zone? This question illustrates that the determination of strain-rate on the basis of microstructures in fault rocks remains a major question, and more comparisons need to be made between experimentally and naturally deformed samples.

Hirabayashi NIED borehole intercepted three fault zones (Tanaka *et al.* 2007 *a*), while the DPRI 1800 borehole intercepted two (Lin *et al.* 2007). Some of these fault zones were activated by the Kobe earthquake, but others were not. As illustrated by the fact it was difficult to identify the principal slip zone of the Kobe earthquake only one year after this event, healing processes may be very efficient and rapidly obliterate the evidence of localised slip. Therefore, we can still ask whether the non-activated faults are locked or inactive? Detailed comparative, collaborative studies by the principal investigators of each of these drill holes are needed to provide more information on the deformation and healing microstructures and mechanisms to address this question.

Nevertheless, the Japanese drill holes through the Nojima Fault have confirmed the international interest in fault zone geology, and progressed the general knowledge on faulting and seismic processes in basement rocks.

## **The Chelungpu Fault (Taiwan)**

### ***General context***

The Chi-Chi earthquake (21 September 1999,  $M_w = 7.6$ , *ca.* 2400 fatalities) produced a surface rupture of 80 km, with up to 10 m offset on the northern part of the Chelungpu thrust fault (Figure 4a, 4b; Kao & Chen 2000). From reconstruction of balanced cross sections, Yue *et al.* (2005) determined that the Sanyi-Chelungpu thrust system has

accommodated 14 km total displacement, and that 0.3 km total slip has been accommodated on a newly propagated North Chelungpu Chinshui detachment within the Chinshui Shale, where the Chi-Chi earthquake occurred (Figure 4b). Thus, in contrast with the Nojima Fault, the Chelungpu Fault has a relatively simple tectonic history.

The Chi-Chi earthquake was recorded by the very dense Taiwan Strong Motion and GPS Networks allowing models of spatial slip distribution (Ma *et al.* 2001), as well as determination of rupture velocity (Chen *et al.* 2001), and of coseismic and postseismic deformation (Pathier *et al.* 2003; Yu *et al.* 2003). During the Chi-Chi earthquake, the northern segment of the Chelungpu Fault was characterized by large displacement (8 to 10m), high slip velocity (2-4m/s) and low level of high-frequency radiation. In contrast, smaller displacement (3-4m), lower slip velocities (0.5m/s) and higher accelerations of the ground motion were measured in the southern part (Ma *et al.* 2003).

Initially, two shallow boreholes penetrated the Chelungpu Fault in March 2001 at 455m (northern site, Fengyuan) and 211m (southern site, Nantou). These provided initial important observations, such as a temperature rise in the northern site on the suspected fault zone activated by the Chi-Chi earthquake (Tanaka *et al.* 2002) and differences in fault zone architecture: clay-rich injections (Otsuki *et al.* 2005; Ujiie 2005) and pseudotachylite fragments (Otsuki *et al.* 2005) are described in the northern and southern boreholes, respectively. As the lithofacies and geological structure are similar at both northern and southern sites, the difference in fault rock microstructures are interpreted as indicating different frictional properties of the fault in these two segments (Otsuki *et al.* 2005; Ujiie *et al.* 2005).

### ***The active fault zone***

The Taiwan Chelungpu Fault Drilling Project (TCDP, Figure 4) was started in 2002. The TCDP site was chosen near the town of DaKeng, about 2 km east of the surface rupture (Figure 4b) in order to allow investigation of the slip-weakening mechanisms responsible for the seismological characteristics of the Chi-Chi earthquake in the northern part of the Chelungpu Fault. Two vertical boreholes were drilled 40 m apart (2000.3 m deep Hole A in 2004 and 1352.6 m deep Hole B in 2005), and a side-track was

drilled from a depth of 950m to 1280m from hole B (hole C in 2005). TCDP holes penetrated through Pliocene and Upper Miocene alternating sandstones, siltstones and shales (Figure 4b; Song *et al.* 2007).

One major feature in the TCDP cores is the colour change of the rocks (from light grey to dark grey, and black) that accompanied deformation. This has been used as a macroscopic on-site criteria for locating fault-zones (Yeh *et al.* 2007). Three major fault zones were recognized in the Chelungpu Fault system in Hole A at 1111, 1153 and 1221m depth (Song *et al.* 2007; Hung *et al.* 2007; Yeh *et al.* 2007; Sone *et al.* 2007) which may correlate to fault zones at 1136, 1194 and 1243m depth, respectively, in Hole B (Figure 4c; Hirono *et al.* 2007). In Hole B the recognition of fault zones was facilitated by the use of systematic non-destructive and continuous measurements performed on the retrieved cores at the Kochi Institute for Core Sample Research (JAMSTEC) such as density, porosity, magnetic susceptibility, natural gamma ray radiation and gamma ray attenuation, magnetic susceptibility and X-ray Computed Tomography (X-ray CT) (Hirono *et al.* 2007). Some, but not all, fault zones also include cm-thick fault-parallel disks of hard black ultracataclasites: at 1153 and 1221m depth in Hole A (Yeh *et al.* 2007) and at 1194, 1243 and 1341m depth in Hole B (Hirono *et al.* 2007).

Among these fault zones, the one located at 1111m in Hole A (FZA1111, Figure 4c) was determined on-site as the fault-zone activated by the Chi-Chi earthquake on the basis of several arguments: high-resolution shallow seismic reflection profiles predicting a depth at 1200m with 10% error; high strain fault kinematics were determined as thrust by fault plane and slickenside orientations consistent with the measured focal mechanism of the Chi-Chi earthquake; high fluid content (Ma *et al.* 2006; Yeh *et al.* 2007; Song *et al.* 2007), fracture density and physical properties measured by logging tools, in particular low resistivity, low density, and distinct Vp and Vs (Hung *et al.* 2007). The total thickness of the FZA1111 fault zone is 5.5m (Yeh *et al.* 2007). It corresponds to the fault zone at 1136m in Hole B (FZB1136, Figure 4c) which has a 3.5m total thickness and is characterized by a lower contrast related to higher permeability on X-ray CT images (Hirono *et al.* 2008).

### ***Energy budget of the earthquake***

One major question arising from the TCDP project concerns the thermal budget of the earthquake, and many papers have been devoted to that point. First, temperature measurements were performed in 2005 in Hole A. A 0.06°C anomaly was found around the FZA1111 (Kano *et al.* 2006), consistent with the 0.1°C anomaly measured earlier in the shallow boreholes (Mori & Tanaka, 2002; Tanaka *et al.* 2006). As discussed by Kano *et al.* (2006) and Tanaka *et al.* (2006, 2007 *b*), the temperature anomaly may occur as (i) residual heat generated during the Chi-Chi earthquake or (ii) may be the result of fluctuations of geothermal gradient related to changes of physical and thermal properties of fault rocks or (iii) be the result of warm fluid upflow in the fault zone due to its high permeability deduced from hydraulic tests (Doan *et al.* 2006) and measurements on core samples (Tanikawa *et al.* 2009). Unfortunately, it is not yet possible to resolve these possibilities in the TCDP boreholes.

Ma *et al.* (2006) calculated the grain size distribution in the very fine-grained gouge recognized as the Chi-Chi PSZ by Kuo *et al.* (2005) in order to better constrain the energy budget of earthquakes. By comparison with the seismic surface fracture energy determined from near-field seismic data, they concluded that the contribution of gouge surface energy represents 6% of the earthquake breakdown work, which is slightly higher than the <1% value obtained on mature Californian faults by Chester *et al.* (2005) and Rockwell *et al.* (2009).

### ***The Chi-Chi PSZ***

The Chi-Chi PSZ was recognized by Kuo *et al.* (2005, 2009) in the lower part of FZA1111 (Figure 5), just above a hard, but fragile black disk, which broke into pieces during on-site core handling. This interpretation was based on the absence of reworking microstructures such as later fractures in the very fine-grained gouge, veins or schistosity and on the presence of smectite as the dominant clay mineral. The authors also observe the presence of glassy material in small quantities (<25%) and suggest that melting of clay minerals due to strong shear heating occurred in the PSZ and that most of the resulting pseudotachylyte was promptly converted into smectite (Kuo *et al.* 2009).

Boullier *et al.* (2009) presented a detailed study of the FZA1111 fault zone, focusing on

the Chi-Chi PSZ. The latter is a 2cm thick, very fine grained, isotropic gouge (Figure 6a) and contains matrix-supported clasts and Clay Clast Aggregates (CCAs, Figure 6b) which are microstructures that have been reproduced by Boutareaud *et al.* (2008, 2010) during high velocity rotary shear experiments where a liquid to vapour transition occurred in the pore water. As such, CCAs are new symptomatic markers of seismic slip in clay-rich gouges, like pseudotachylytes are in "hard" rocks (Sibson 1975). Clasts of the lower black ultracataclasites are also present in the PSZ and display an inverse grain size segregation according to the Brazil Nut Effect (Boullier *et al.* 2009). All these microstructural criteria lead Boullier *et al.* (2009) to propose that the gouge was fluidized as the result of a 300-400°C coseismic temperature rise inducing thermal pressurization (Sibson 1973). This phenomenon may explain the gouge injections observed above the FZA1111 (Figure 5) and in the northern shallow borehole (Otsuki *et al.* 2005; Ujiie 2005). The Chi-Chi PSZ in FZB1136 is very different from the PSZ in FZA1111; it is a thin (<0.3 cm versus 2 cm) ultracataclasite, locally exhibiting a layering defined by variations in concentrations of clay minerals and clasts (Boullier *et al.* 2009) similar to foliated gouges experimentally reproduced by Boutareaud *et al.* (2008) and Mizoguchi *et al.* (2009).

Continuous in-situ and non-destructive measurement of the magnetic susceptibility in Hole B has shown that fault zones, and FZB1136 in particular, are characterized by an important increase of the magnetic susceptibility which has been interpreted by Hirano *et al.* (2006) as due to the production of ferrimagnetic iron oxydes induced by frictional heat as experimentally reproduced during high-speed frictional testings (Fukuchi *et al.* (2005). Recently, Chou *et al.* (2009, 2010) and Aubourg *et al.* (2010) performed a very detailed and complete analysis of magnetic properties on FZB1136 using a U-channel sample. They measured the magnetic susceptibility, the isothermal remanent magnetization and S-ratio, and the anhysteretic remanent magnetization every cm, together with low-temperature magnetic properties to identify the magnetic minerals. Their measurements have been precisely compared with microstructures described by Boullier *et al.* (2009). The principal results are as follows: (i) a paleomagnetic component close to the modern dipole is recovered all along the FZB1136, (ii) very small amounts of fine-grained magnetite and pyrrhotite constitute the magnetic assemblage in the PSZ, and (iii) authigenic goethite has been clearly identified by TEM in and above the PSZ and attributed to circulation and post-seismic cooling of hot fluids in



the FZB1136 (Chou *et al.* 2009, 2010; Aubourg *et al.* 2010). Therefore, they confirm that frictional heating occurred in the Chi-Chi PSZ.

Through measurement of major and trace element chemistry, as well as isotope ratios of core samples, Ishikawa *et al.* (2008) illustrated that the three fault zones exhibit sharp compositional peaks of fluid-mobile elements and strontium isotopes. They suggest that coseismic hot ( $>350^{\circ}\text{C}$ ) fluids circulated and interacted with the fault rocks where they mobilized these elements. Hashimoto *et al.* (2008) attribute the low iron content of chlorite in the fault zone to result from a temperature rise and rock-fluid interactions in the three fault zones (FZB1136, FZB1194 and FZB1243). All these results are consistent with the magnetic characteristics of FZB1136 quoted above.

Coseismic rise of temperature in the fault zones has been documented in a number of other publications about the TCDP. Because the hard disks of black ultracataclasites are noticeable feature of the TCDP core samples, they have been investigated using different methods. Hirono *et al.* (2006) have shown that the anomalies in magnetic susceptibility measured on the black ultracataclasites in FZB1194 and FZB1243 coincide with the evidence for frictional melt and a decrease in inorganic carbon that they attribute to thermal decomposition of carbonate minerals at ca.  $850^{\circ}\text{C}$ . However, the effect of thermal decomposition of carbonates may be very complex if the mass and energy balance, and the kinetics of the endothermic reaction of calcite decomposition, are taken into account (Sulem & Famin, 2009). Otsuki *et al.* (2009) confirm that the hard black disks correspond to pseudotachylytic layers indicative of a single (FZB1314) or multiple (FZB1194, FZB1243) seismic events, and that co-seismic temperature rise has been heterogeneous in the pseudotachylytic layer and may be estimated in the  $750^{\circ}$  to  $1750^{\circ}\text{C}$  range.

In conclusion, although different authors agree frictional heating occurred on fault zones in the Chelungpu Fault, they propose different values for the temperature rise. It appears that the coseismic thermal rise was around  $300\text{--}400^{\circ}\text{C}$  in the Chi-Chi PSZ in FZA1111 and FZB1136 (Ishikawa *et al.* 2008; Boullier *et al.* 2009) and may have reached  $750^{\circ}\text{C}$  or more in the hard disks of black ultracataclasites observed in Hole B on FZB1194 and FZB1243 fault zones which correspond to ancient seismic events (Hirono *et al.* 2006; Otsuki *et al.* 2009).

Several gouge layers corresponding to ancient seismic events are visible in the FZA1111

and FZB1136. They differ from the PSZ because they display a sequence of small conjugate shear zones, a fault-parallel schistosity associated with deformed calcite veins, both being folded together in some places, and dissolution seams around hard objects (Boullier *et al.* 2009). These microstructures are consistent with a fault-normal shortening and are symptomatic of a low-rate deformation by dissolution-precipitation processes which occur during the post-seismic or the interseismic stage (Gratier & Gueydan, 2007).

### ***Fluids: before, during and after earthquakes***

Boullier *et al.* (2009) described thin calcite veins above the Chi-Chi PSZ in FZA1111 within compacted gouges, which form 3D dilational patches and display evidence of increasing strain with increasing distance from the PSZ. They were formed by hydraulic fracturing, and are undeformed just above the PSZ where they are interpreted by Boullier *et al.* (2009) as induced by fluid escape, fracturing and sealing related to the Chi-Chi earthquake. Farther from the PSZ, veins are planar or shortened and folded, and orientated at high angle to the fault. In the damage zone, the silty and sandy layers are dilated, fractured and sealed by calcite while shaly layers are not. This suggests that clay-rich layers may have acted as impermeable caps allowing compartmentalization of fluids in the sandy sediments and formation of small-size so-called "Hill fault/fracture-meshes" (Sibson 1994).

It has been shown earlier that fluids played an important role during the Chi-Chi earthquake because they have been coseismically thermally pressurized. However, the relative scarcity of calcite veins in the active damage zone compared to the large volume of laumontite and carbonate veins in the Nojima Fault demonstrates that the volumes of fluids involved in deformation on the Chelungpu Fault are much smaller than those involved in the Nojima Fault. Regardless, their role in the Chelungpu faulting process illustrates that fluids may greatly influence the seismological behaviour of faults even if they are present in small quantities.

### ***Lessons from the Taiwan Chelungpu Fault Drilling Project.***

One major lesson from the TCDP project concerns the thermal budget of an earthquake. In order to measure frictional heat arising from the fault slip, the temperature must be measured in the vicinity of the PSZ as quickly and as deep as possible after an earthquake (Brodsky *et al.* 2009). However, observations from the TCDP illustrate that part of the frictional heat produced by the earthquake may be transformed into mechanical (thermal pressurization) and chemical (mineral transformations, fluid-rock interactions) work. One major contribution of TCDP to earthquake understanding has been the demonstration that the energy budget of an earthquake cannot be separated into simple fracturing, radiation and thermal terms but should also take into account chemical and mineralogical transformations.

As the Chelungpu Fault occurs in sedimentary rocks made of alternating silts and shales, clays are important minerals within the fault zone. The TCDP results show that the behaviour of clays during co-seismic slip is fundamental in order to understand slip-weakening mechanisms. Therefore, for the same reasons that the Japanese drilling projects have stimulated experiments on "hard" rocks, the TCDP project has stimulated high velocity rotary shear friction experiments on "soft" rocks from the Chelungpu Fault (Mizoguchi *et al.* 2008 *b*; Tanikawa & Shimamoto 2009; Sone & Shimamoto 2009) and numerical modelling of the thermal pressurization related to dehydration of clays (Sulem *et al.* 2007). The high-velocity experiments on clayey gouges have produced microstructures that have been recognized in the Chi-Chi PSZ and are keys for interpreting natural fault gouges. For example, Clay Clast Aggregates (CCAs); new indicators for seismic slip, thermal pressurization and slip weakening have been described (Boutareaud *et al.* 2008, 2010).

The studies undertaken on the TCDP samples have demonstrated that the mineralogy of the PSZ is of considerable importance and that chemical and mineralogical transformations may occur in the PSZ due to the frictional heat produced there. However, the proposed values for the frictional heat differ significantly between different publications. The effect of thermal decomposition of minerals may be very complex and to model its mechanical effects such as slip weakening due to thermal pressurization it is necessary to take into account the mass and energy balance and the kinetics of the chemical decomposition (Sulem & Famin 2009).

Again, the distribution of physical properties, and transport properties in particular,

within the core and the damage zones of the fault is of primary importance to understand the coseismic slip behaviour of the PSZ and thermal pressurization in particular. The permeability structure of the Chelungpu Fault has been investigated in several studies using the TCDP samples (Tanikawa *et al.* 2009; Wang *et al.* 2009; Chen *et al.* 2009; Louis *et al.* 2008) which have demonstrated that drilling projects through active faults should include such measurements. To do so, core handling is of primary importance. The core-handling workflows were different for Hole A and Hole B samples. The results of continuous non-destructive analyses performed on Hole B samples only, were made available a short time after drilling. However, it has been shown that these rock analyses are not sufficient and that detailed studies are necessary to provide precise information on microstructures and mineralogy. For example, whole-rock analyses pointed to the fact that there is an important magnetic susceptibility record in the black ultracataclasites, that may be significant in terms of mineral transformations and thermal pressurization (Hirono *et al.* 2006). However, only detailed subsequent investigations have deciphered the exact nature of this magnetic signal and shown that the Chi-Chi PSZ records the present-day Earth's magnetic field (Chou *et al.* 2010). TCDP has led to numerous analyses of magnetic properties of fault rocks which contributed to the development of new techniques and approaches of the fault zone geology.

The work done on the TCDP so far represents significant progress in understanding fault zone processes, but we still need more information on clay mineralogy, composition and volume of pore fluids before and after the earthquake, in order to fully understand the mechanical and slip-weakening effects of mineral transformations in the PSZ.

Regardless, the numerous studies on TCDP samples have contributed to a better knowledge of thrust faults in clay-rich rocks and, consequently, have provided good preparation for the international community for other drilling projects such as NanTroSeize in the Nankai Trough.

## Conclusions

This paper has focussed on the contributions of the Japanese and Taiwanese drilling projects to a better knowledge of the geology of fault zones. Some results have probably been missed as it is impossible to cite all the papers published on the subject. Each

project has provided its own unique set of results because the faults crosscut different parent rocks and occur in different geodynamic and tectonic contexts. Consequently, different processes and deformation mechanisms have been activated during earthquakes on the Nojima and Chelungpu faults. In addition, large volumes of fluids were involved in the alteration of the Nojima wallrocks while only small volumes of fluids were present in the Chelungpu Fault system. This illustrates that there is no unique process applicable to all faults around the world. Fortunately, other projects are in progress that will investigate other fault types: the San Andreas Fault Observatory at Depth (SAFOD) in Parkfield (California), the Wenchuan earthquake Fault Scientific Drilling (WFSD) through the Longmen Shan active fault zone (China), the NanTroSeize project through the Nankai accretionary prism and subduction zone and the Deep Fault Drilling Project (DFDP) through the Alpine Fault (New Zealand). With the help of these projects combined with surface studies, we can expect to obtain some answers to remaining questions.

Drilling projects, although not the only way to do so, have been performed to understand earthquakes as large-scale phenomena recorded by seismologists and have triggered many micro-scale studies that have led to a better knowledge of the Principal Slip Zone which controls the seismological behaviour of faults during earthquakes (Sibson 2003). Thus, questions at a macroscale have stimulated research at a microscale. Reciprocally, answers provided from micro-scale studies have explained some macroscopic behaviours of active faults. We may cite as an example the recognition of thermal pressurization in the Chi-Chi PSZ which explains the peculiar seismic behaviour of the northern segment of the Chelungpu Fault during the Chi-Chi earthquake.

Let us reconsider the objectives of drilling projects through active faults (Zoback *et al.* 2007) designed "to directly study the physical and chemical processes that control deformation and earthquake generation within active fault zones". It is apparent that we still need information on the thermal signature and heat production of earthquakes, the pressure and composition of pore fluid, the healing processes and their kinetics, and the mechanisms of aseismic creep on faults. On-going and future drilling projects through active faults will certainly improve our knowledge, and provide supplementary information to address these questions by stimulating intense and fruitful collaborations between geologists and seismologists.

699

700 **Acknowledgements**

701 The author thanks her Japanese (K. Fujimoto, H. Ito, T. Ohtani) and Taiwanese (Y.-M.  
702 Chou, L.-W. Kuo, T.-K. Lee, S.-R. Song, E.-C. Yeh) colleagues for allowing her to  
703 collaborate with them on the fantastic and precious samples from the Hirabayashi and  
704 TCDP boreholes. These studies of the geology of fault zones are part of more  
705 comprehensive projects with French colleagues and have been financially supported by  
706 the CNRS and/or Ministère des Affaires Etrangères (PICS 1050 France-Japon, PAI  
707 ORCHID 2006, International Laboratory CNRS-NSC France-Taiwan ADEPT) and by ANR  
708 (ACTS Taiwan, ANR-06-CATT-001-01). AMB thanks also Michel Bouchon for critically  
709 reading a first draft of this manuscript, Toshi Shimamoto for his constructive review and  
710 Virginia Toy for her help in making the message clearer. Last but not least, she is grateful  
711 to Rick Sibson for advising and encouraging her every time she met him in Europe,  
712 North America or New Zealand for discussions on mylonites, pseudotachylytes, gold  
713 mines, earthquakes, birds, history, poetry and many other subjects.

714

715 **References**

- 716 Aubourg, C., Chou, Y.-M., Song, S. R., Boullier, A. M. & Lee, C. T. 2010. A new portrait of mm-thick  
717 principal slip zone of the ChiChi earthquake (Mw 7.6; 1999). In: *Western Pacific Geophysical*  
718 *Meeting. Suppl.* **91(26)**, Taipei, Taiwan, Abstract T33B-03.
- 719 Awata, Y. & Mizuno, K. 1998. Strip map of the surface fault ruptures associated with the 1995  
720 Hyogo-ken Nanbu earthquake, central Japan - the Nojima, Ogura and Nadagawa earthquake  
721 faults. Geological Survey of Japan, Tsukuba.
- 722 Blenkinsop, T. G. & Sibson, R. H. 1992. Aseismic fracturing and cataclasis involving reaction  
723 softening within core material from the Cajon Pass drill hole. *Journal of Geophysical Research*  
724 **97(B4)**, 5135-5144.
- 725 Bouchon, M., Sekiguchi, H., Irikura, K. & Iwata, T. 1998. Some characteristics of the stress field of  
726 the 1995 Hyogo-ken Nanbu (Kobe) earthquake. *Journal of Geophysical Research* **103**, 24271-  
727 24282.
- 728 Boullier, A. M., Ohtani, T., Fujimoto, K., Ito, H. & Dubois, M. 2001. Fluid inclusions in  
729 pseudotachylytes from the Nojima Fault, Japan. *Journal of Geophysical Research-Solid Earth*  
730 **106(B10)**, 21965-21977.
- 731 Boullier, A. M., Fujimoto, K., Ito, H., Ohtani, T., Keulen, N., Fabbri, O., Amitrano, D., Dubois, M. &  
732 Pezard, P. 2004 a. Structural evolution of the Nojima Fault (Awaji Island, Japan) revisited  
733 from the GSJ drill hole at Hirabayashi. *Earth Planets and Space* **56(12)**, 1233-1240.
- 734 Boullier, A. M., Fujimoto, K., Ohtani, T., Roman-Ross, G., Lewin, E., Ito, H., Pezard, P. & Ildefonse, B.  
735 2004 b. Textural evidence for recent co-seismic circulation of fluids in the Nojima Fault zone,  
736 Awaji island, Japan. *Tectonophysics* **378(3-4)**, 165-181.

- 737 Boullier, A. M., Yeh, E. C., Boutareaud, S., Song, S. R. & Tsai, C. H. 2009. Microscale anatomy of the  
738 1999 Chi-Chi earthquake fault zone. *Geochemistry Geophysics Geosystems* **10**, 3, Q03016,  
739 doi:10.1029/2008GC002252.
- 740 Boutareaud, S., Calugaru, D. G., Han, R., Fabbri, O., Mizoguchi, K., Tsutsumi, A. & Shimamoto, T.  
741 2008. Clay-clast aggregates: a new structural evidence for seismic fault sliding? *Geophysical*  
742 *Research Letters* **35**, L05302, doi:10.1029/2007GL032554.
- 743 Boutareaud, S., Boullier, A. M., Andreani, M., Calugaru, D. G., Beck, P., Song, S. R. & Shimamoto, T.  
744 2010. Clay clast aggregates in gouges: New textural evidence for seismic faulting. *Journal of*  
745 *Geophysical Research-Solid Earth* **115**, B02408, doi:10.1029/2008JB006254.
- 746 Brodsky, E. E., Ma, K.-F., Mori, J., Saffer, D. & and the participants of the ICDP/SCEC International  
747 Workshop. 2009. Rapid Reponse Fault Drilling: Past, Present and Future. *Scientific Drilling* **8**,  
748 66-74.
- 749 Caine, J., Evans, J. & Forster, C. 1996. Fault zone architecture and permeability structure. *Geology*  
750 **26**(11), 1025-1028.
- 751 Célérrier, B. P., Pezard, P. A., Ito, H. & Kiguchi, T. 2000. Borehole wall geometry across the Nojima  
752 Fault: BHTV acoustic scans analysis from the GSJ Hirabayashi Hole, Japan. In: *International*  
753 *workshop of the Nojima Fault core and borehole data analysis* (edited by Ito, H., Fujimoto, K.,  
754 Tanaka, H. & Lockner, D.) **GSJ Interim report No.EQ/00/1, USGS Open-File Report 000-**  
755 **129**. Geological Survey of Japan, Tsukuba, Japan, 233-238.
- 756 Chen, K. C., Huang, B. S., Wang, J. H., Huang, W. G., Chang, T. M., Hwang, R. D., Chiu, H. C. & Tsai, C.  
757 C. P. 2001. An observation of rupture pulses of the 20 September 1999 Chi-Chi, Taiwan,  
758 earthquake from near-field seismograms. *Bulletin of the Seismological Society of America*  
759 **91**(5), 1247-1254.
- 760 Chen, T. M. N., Zhu, W. L., Wong, T. F. & Song, S. R. 2009. Laboratory Characterization of  
761 Permeability and Its Anisotropy of Chelungpu Fault Rocks. *Pure and Applied Geophysics*  
762 **166**(5-7), 1011-1036.
- 763 Chester, J. S., Chester, F. M. & Kronenberg, A. K. 2005. Fracture surface energy of the Punchbowl  
764 Fault, San Andreas system. *Nature* **437**(7055), 133-136.
- 765 Chou, Y.-M., Lee, T.-Q., Aubourg, C., Boullier, A. M. & Song, S.-R. 2009. Magnetic mineralogy and its  
766 correspondence with SEM observations on FZB1136 fault gouge of the Chi-Chi earthquake,  
767 Chelungpu Fault, Taiwan. In: *EGU General Assembly* **11**, Vienna, Abstract EGU2009-5950.
- 768 Chou, Y.-M., Song, S. R., Aubourg, C., Lee, C. T. & Yeh, E. C. 2010. The paleomagnetic record of Chi-  
769 Chi earthquake (Mw 7.6, 1999). In: *Western Pacific Geophysical Meeting. Suppl.* **91**(26),  
770 Taipei, Taiwan, Abstract T31A-061.
- 771 Di Toro, G., Goldsby, D. L. & Tullis, T. E. 2004. Friction falls toward zero in quartz rock as slip  
772 velocity approaches seismic rates. *Nature* **427**, 436-439.
- 773 Di Toro, G. & Pennacchioni, G. 2004. Superheated friction-induced melts in zoned  
774 pseudotachylytes within the Adamello tonalites (Italian Southern Alps). *Journal of Structural*  
775 *Geology* **26**(10), 1783-1801.
- 776 Doan, M. L., Brodsky, E. E., Kano, Y. & Ma, K. F. 2006. In situ measurement of the hydraulic  
777 diffusivity of the active Chelungpu Fault, Taiwan. *Geophysical Research Letters* **33**(L16317),  
778 doi:10.1029/2006GL026889.

- 779 Doan, M. L. & Gary, G. 2009. Rock pulverization at high strain rate near the San Andreas Fault.  
780 *Nature Geoscience* **2**(10), 709-712.
- 781 Dor, O., Ben-Zion, Y., Rockwell, T. K. & Brune, J. 2006. Pulverized rocks in the Mojave section of  
782 the San Andreas Fault Zone. *Earth and Planetary Science Letters* **245**(3-4), 642-654.
- 783 Fabbri, O., Iwamura, K., Matsunaga, S., Coromina, G. & Kanaori, Y. 2004. Distributed strike-slip  
784 faulting, block rotation, and possible intracrustal vertical decoupling in the convergent zone  
785 of southwest Japan. In: *Vertical Coupling and Decoupling of the Lithosphere* (edited by Grocott,  
786 J., Tikoff, B., McCaffrey, K. J. W. & Taylor, G.) **227**. Geological Society, London, Special  
787 Publications, 141-166.
- 788 Famin, V., Nakashima, S., Boullier, A. M., Fujimoto, K. & Hirono, T. 2008. Earthquakes produce  
789 carbon dioxide in crustal faults. *Earth and Planetary Science Letters* **265**(3-4), 487-497.
- 790 Fujimoto, K., Tanaka, H., Higuchi, T., Tomida, N., Ohtani, T. & Ito, H. 2001. Alteration and mass  
791 transfer inferred from the Hirabayashi GSJ drill penetrating the Nojima Fault, Japan. *The*  
792 *Island Arc* **10**(3-4), 401-410.
- 793 Fujimoto, K., Ueda, A., Ohtani, T., Takahashi, M., Ito, H., Tanaka, H. & Boullier, A.-M. 2007.  
794 Borehole water and hydrologic model around the Nojima Fault, SW Japan. *Tectonophysics*  
795 **443**, 174-182.
- 796 Fukuchi, T. & Imai, N. 2001. ESR and ICP analyses of the DPRI 500 m drill core samples  
797 penetrating through the Nojima Fault, Japan. *The Island Arc* **10**(3-4), 465-478.
- 798 Fukuchi, T., Mizoguchi, K. & Shimamoto, T. 2005. Ferrimagnetic resonance signal produced by  
799 frictional heating: A new indicator of paleoseismicity. *Journal of Geophysical Research-Solid*  
800 *Earth* **110**(B12), B12404, doi:10.1029/2004JB003485.
- 801 Gratier, J. P., Favreau, P. & Renard, F. 2003. Modeling fluid transfer along California faults when  
802 integrating pressure solution crack sealing and compaction processes. *Journal of Geophysical*  
803 *Research* **108**(B2), 28-52.
- 804 Gratier, J. P. & Gueydan, F. 2007. Deformation in the presence of fluids and mineral reactions:  
805 effect of fracturing and fluid-rocks interaction on seismic cycle. In: *Tectonic faults, agents of*  
806 *change on a dynamic earth* (edited by Handy, M. R., Hirth, G. & Hovius, N.). *Dahlem workshop*  
807 *reports*. The MIT Press, Cambridge, Mass., USA, 319-356.
- 808 Hashimoto, Y., Tadaï, O., Tanimizu, M., Tanikawa, W., Hirono, T., Lin, W., Mishima, T., Sakaguchi,  
809 M., Soh, W., Song, S.-R., Aoike, K., Ishikawa, T., Murayama, M., Fujimoto, K., Fukuchi, T.,  
810 Ikehara, M., Ito, H., Kikuta, H., Kinoshita, M., Masuda, K., Matsubara, T., Matsubayashi, O.,  
811 Mizoguchi, M., Nakamura, N., Otsuki, K., Shimamoto, T., Sone, H. & Takahashi, M. 2008.  
812 Characteristics of chlorites in seismogenic fault zones: the Taiwan Chelungpu Fault Drilling  
813 Project (TCDP) core sample. *e-Earth* **3**(<http://www.electronic-earth.net/3/issue1.html>), 1-6.
- 814 Hickman, S., Sibson, R. H. & Bruhn, R. 1995. Introduction to special section: Mechanical  
815 involvement of fluids in faulting. *Journal of Geophysical Research* **100**(B7), 12831-12840.
- 816 Hirono, T., Lin, W. R., Yeh, E. C., Soh, W., Hashimoto, Y., Sone, H., Matsubayashi, O., Aoike, K., Ito,  
817 H., Kinoshita, M., Murayama, M., Song, S. R., Ma, K. F., Hung, J. H., Wang, C. Y. & Tsai, Y. B. 2006.  
818 High magnetic susceptibility of fault gouge within Taiwan Chelungpu Fault: Nondestructive  
819 continuous measurements of physical and chemical properties in fault rocks recovered from  
820 Hole B, TCDP. *Geophysical Research Letters* **33**(15), L15303, doi:10.1029/2006GL026133.
- 821 Hirono, T., Yeh, E. C., Lin, W., Sone, H., Mishima, T., Soh, W., Hashimoto, Y., Matsubayashi, O.,  
822 Aoike, K., Ito, H., Kinoshita, M., Murayama, M., Song, S. R., Ma, K. F., Hung, J. H., Wang, C. Y.,



- 823 Tsai, Y. B., Kondo, T., Nishimura, M., Moriya, S., Tanaka, T., Fujiki, T., Maeda, L., Muraki, H.,  
824 Kuramoto, T., Sugiyama, K. & Sugawara, T. 2007. Non-destructive continuous physical  
825 property measurements of core samples recovered from hole B, Taiwan Chelungpu-Fault  
826 Drilling Project. *Journal of Geophysical Research* **112**, B07404, doi:10.1029/2006JB004738.
- 827 Hirono, H., Sakaguchi, M., Otsuki, K., Sone, H., Fujimoto, K., Mishima, T., Lin, W., Tanikawa, W.,  
828 Tanimizu, M., Soh, W., Yeh, E. C. & Song, S. R. 2008. Characterization of slip zone associated  
829 with the 1999 Taiwan Chi-Chi earthquake: X-ray CT image analyses and microstructural  
830 observations of the Taiwan Chelungpu Fault. *Tectonophysics* **449**, 63-84, doi:  
831 10.1016/j.tecto.2007.12.002.
- 832 Hirose, T. & Shimamoto, T. 2005. Growth of molten zone as a mechanism of slip weakening of  
833 simulated faults in gabbro during frictional melting. *Journal of Geophysical Research-Solid*  
834 *Earth* **110**(B5), B05202, doi:10.1029/2004JB003207.
- 835 Hung, J. H., Wu, Y. H., Yeh, E. C., Wu, J. C. & Party, a. T. S. 2007. Subsurface structure, physical  
836 properties, and fault zone characteristics in the scientific drill holes of Taiwan Chelungpu-  
837 Fault Drilling Project. *Terrestrial, Atmospheric and Oceanic Sciences* **18**(2), 271-293.
- 838 Ikeda, R. 2001. Outline of the fault zone drilling project by NIED in the vicinity of the 1995  
839 Hyogo-ken Nanbu earthquake, Japan. *The Island Arc* **10**(3-4), 199-205.
- 840 Irikura, K., Iwata, T., Sekiguchi, H., Pitarka, A. & Kamae, K. 1996. Lesson from the 1995 Hyogo-  
841 Ken Nanbu earthquake: Why were such destructive motions generated to buildings? *J. Nat.*  
842 *Disaster Sci.* **17**, 99-127.
- 843 Ishikawa, T., Tanimizu, M., Nagaishi, K., Matsuoka, J., Tadaï, O., Sakaguchi, M., Hirono, T., Mishima,  
844 T., Tanikawa, W., Lin, W., Kikuta, H., Soh, W. & Song, S. R. 2008. Coseismic fluid-rock  
845 interactions at high temperatures in the Chelungpu Fault. *Nature Geoscience* **1**(10), 679-683.
- 846 Ito, H., Kuwahara, T., Miyazaki, O., Kiguchi, T., Fujimoto, K., Ohtani, T., Tanaka, H., Higuchi, S.,  
847 Agar, S., Brie, A. & Yamamoto, H. 1996. Structure and physical properties of the Nojima Fault  
848 (in Japanese with English abstract). *BUTSURI-TANSA (Geophysical Exploration)* **49**, 522-535.
- 849 Ito, H. & Kiguchi, T. 2005. Distribution and properties of fractures in and around the Nojima  
850 Fault in the Hirabayashi GSJ borehole. In: *Petrophysical properties of crystalline rocks* (edited  
851 by Harvey, P. K., Brewer, T. S., Pezard, P. A. & Petrov, V. A.) **240**. Geological Society, London,  
852 Special Publications, 61-74.
- 853 Kanamori, H. & Heaton, T. H. 2000. Microscopic and macroscopic physics of earthquakes. In:  
854 *GeoComplexity and the Physics of Earthquakes* (edited by Rundle, J., Turcotte, D. L. & Klein,  
855 W.). *Geophysical Monograph*. American Geophysical Union, 147-163.
- 856 Kanaori, Y. 1990. Late Mesozoic-Cenozoic strike-slip and block rotation in the inner belt of  
857 Southwest Japan. *Tectonophysics* **177**, 381-399.
- 858 Kano, Y., Mori, J., Fujio, R., Ito, H., Yanagidani, T., Nakao, S. & Ma, K.-F. 2006. Heat signature on the  
859 Chelungpu Fault associated with the 1999 Chi-Chi, Taiwan earthquake. *Geophysical Research*  
860 *Letters* **33**, L14306, doi:10.1029/2006GL026733.
- 861 Kao, H. & Chen, W. P. 2000. The Chi-Chi earthquake sequence: active out-of-sequence thrust  
862 faulting in Taiwan. *Science* **288**, 2346-2349.
- 863 Keulen, N., Heilbronner, R., Stuenitz, H., Boullier, A. M. & Ito, H. 2007. Grain size distributions of  
864 fault rocks: A comparison between experimentally and naturally deformed granitoids. *Journal*  
865 *of Structural Geology* **29**(8), 1282-1300.

- 866 Keulen, N., Stunitz, H. & Heilbronner, R. 2008. Healing microstructures of experimental and  
867 natural fault gouge. *Journal of Geophysical Research-Solid Earth* **113**, B06205,  
868 doi:10.1029/2007JB005039.
- 869 Kiguchi, T., Ito, H., Kuwahara, Y. & Miyazaki, T. 2001. Estimating the permeability of the Nojima  
870 Fault Zone by a hydrophone vertical seismic profiling experiment. *The Island Arc* **10**(3-4),  
871 348-356.
- 872 Kitajima, T., Kobayashi, Y., Ikeda, R., Iio, Y. & Omura, K. 1998. Terrestrial heat flow in Nojima-  
873 Hirabayashi, Awaji Island. *Chikyu Monthly (in Japanese)* **21**, 108-113.
- 874 Kobayashi, K., Hirano, S., Arai, T., Ikeda, R., Omura, K., Sano, H., Sawaguchi, T., Tanaka, H., Tomita,  
875 T., Tomida, N., Matsuda, T. & Yamazaki, A. 2001. Distribution of fault rocks in the fracture  
876 zone of the Nojima Fault at a depth of 1140 m: Observations from the Hirabayashi NIED drill  
877 core. *The Island Arc* **10**(3-4), 411-421.
- 878 Kuo, L. W., Song, S. R. & Chen, H. Y. 2005. Characteristics of clay mineralogy in the fault zone of  
879 the TCDP and its implication. *Eos Trans. AGU, Fall Meet. Supp.* **86**(52), Abstract T43D-05.
- 880 Kuo, L.-W., Song, S.-R., Yeh, E.-C. & Chen, H.-F. 2009. Clay mineral anomalies in the fault zone of  
881 the Chelungpu Fault, Taiwan, and their implications. *Geophysical Research Letters* **36**, L18306,  
882 doi:10.1029/2009GL039269.
- 883 Lin, A. M., Shimamoto, T., Maruyama, T., Sigetomi, M., Miyata, T., Takemura, K., Tanaka, H., Uda, S.  
884 & Murata, A. 2001. Comparative study of cataclastic rocks from a drill core and outcrops of  
885 the Nojima Fault zone on Awaji Island, Japan. *The Island Arc* **10**(3-4), 368-380.
- 886 Lin, A., Tanaka, N., Uda, S. & Satish-Kumar, M. 2003. Repeated coseismic infiltration of meteoric  
887 and seawater into deep fault zones: a case study of the Nojima Fault zone, Japan. *Chemical*  
888 *Geology* **202**(1-2), 139-153.
- 889 Lin, A., Maruyama, T. & Kobayashi, K. 2007. Tectonic implications of damage zone-related fault-  
890 fracture networks revealed in drill core through the Nojima Fault, Japan. *Tectonophysics*  
891 **443**(3-4), 161-173.
- 892 Lockner, D. A., Tanaka, H., Ito, H., Ikeda, R., Omura, K. & Naka, H. 2009. Geometry of the Nojima  
893 Fault at Nojima-Hirabayashi, Japan - I. A Simple Damage Structure Inferred from Borehole  
894 Core Permeability. *Pure and Applied Geophysics* **166**(10-11), 1649-1667.
- 895 Louis, L., Chen, T. M. N., David, C., Robion, P., Wong, T. F. & Song, S. R. 2008. Anisotropy of  
896 magnetic susceptibility and P-wave velocity in core samples from the Taiwan Chelungpu-  
897 Fault Drilling Project (TCDP). *Journal of Structural Geology* **30**(8), 948-962.
- 898 Ma, K. F., Mori, J., Lee, S. J. & Yu, S. B. 2001. Spatial and temporal distribution of slip for the 1999  
899 Chi-Chi, Taiwan earthquake. *Bulletin of the Seismological Society of America* **91**(5), 1069-  
900 1087.
- 901 Ma, K. F., Brodsky, E. E., Mori, J., Ji, C., Song, T. R. A. & Kanamori, H. 2003. Evidence for fault  
902 lubrication during the 1999 Chi-Chi, Taiwan, earthquake (Mw7.6). *Geophysical Research*  
903 *Letters* **30**(5), 1244, doi:10.1029/2002GL015380.
- 904 Ma, K. F., Tanaka, H., Song, S. R., Wang, C. Y., Hung, J. H., Tsai, Y. B., Mori, J., Song, Y. F., Yeh, E. C.,  
905 Soh, W., Sone, H., Kuo, L. W. & Wu, H. Y. 2006. Slip zone and energetics of a large earthquake  
906 from the Taiwan Chelungpu-Fault Drilling Project. *Nature* **444**(23 November), 473-476,  
907 doi:10.1038/nature05253.

- 908 Matsuda, T., Arai, T., Ikeda, R., Omura, K., Kobayashi, K., Sano, H., Sawaguchi, T., Tanaka, H.,  
909 Tomita, T., Tomida, N., Hirano, S. & Ymazaki, A. 2001. Examination of mineral assemblage and  
910 chemical composition in the fracture zone of the Nojima Fault at a depth of 1140 m: Analyses  
911 of the Hirabayashi NIED drill cores. *The Island Arc* **10**(3-4), 422-429.
- 912 Matsuda, T., Omura, K., Ikeda, R., Arai, T., Kobayashi, K., Shimada, K., Tanaka, H., Tomita, T. &  
913 Hirano, S. 2004. Fracture-zone conditions on a recently active fault: insights from  
914 mineralogical and geochemical analyses of the Hirabayashi NIED drill core on the Nojima  
915 Fault, southwest Japan, which ruptured in the 1995 Kobe earthquake. *Tectonophysics* **378**(3-  
916 4), 143-163.
- 917 Mitchell, T. M., Shimamoto, T. & Ben-Zion, Y. 2009. Pulverized Fault Rocks and Damage  
918 Asymmetry along the Arima-Takatsuki Tectonic Line, Japan: Fault Structure, Damage  
919 Distribution and Textural Characteristics. In: *Fall Meeting*. American Geophysical Union,  
920 abstract #T54A-02.
- 921 Mizoguchi, K., Hirose, T., Shimamoto, T. & Fukuyama, E. 2008 a. Internal structure and  
922 permeability of the Nojima Fault, southwest Japan. *Journal of Structural Geology* **30**(4), 513-  
923 524.
- 924 Mizoguchi, K., Takahashi, M., Tanikawa, W., Masuda, K., Song, S. R. & Soh, W. 2008 b. Frictional  
925 strength of fault gouge in Taiwan Chelungpu Fault obtained from TCDP Hole B.  
926 *Tectonophysics* **460**(1-4), 198-205.
- 927 Mizoguchi, K., Hirose, T., Shimamoto, T. & Fukuyama, E. 2009. High-velocity frictional behavior  
928 and microstructure evolution of fault gouge obtained from Nojima Fault, southwest Japan.  
929 *Tectonophysics* **471**(3-4), 285-296.
- 930 Moore, D. E., Lockner, D. A., Ito, H., Ikeda, R., Tanaka, H. & Omura, K. 2009. Geometry of the  
931 Nojima Fault at Nojima-Hirabayashi, Japan - II. Microstructures and their Implications for  
932 Permeability and Strength. *Pure and Applied Geophysics* **166**(10-11), 1669-1691.
- 933 Mori, J. & Tanaka, H. 2002. Energy budget of the 1999 Chichi, Taiwan earthquake. In: *Fall*  
934 *Meeting Suppl.* **83**(7). Eos Trans. AGU, Abstract S71E-09.
- 935 Murakami, M., Tagami, T. & Hasebe, N. 2002. Ancient thermal anomaly of an active fault system:  
936 Zircon fission-track evidence from Nojima GSJ 750 m borehole samples. *Geophysical Research*  
937 *Letters* **29**(23), B05202, doi:10.1029/2004JB003207.
- 938 Murakami, M. & Tagami, T. 2004. Dating pseudotachylite of the Nojima Fault using the zircon  
939 fission-track method. *Geophysical Research Letters* **31**(12), L12604,  
940 doi:10.1029/2004GL020211.
- 941 Murata, A., Takemura, K., Miyata, T. & Lin, A. 2001. Quaternary vertical offset and average slip  
942 rate of the Nojima Fault on Awaji Island, Japan. *The Island Arc* **10**, 360-367.
- 943 Ohtani, T., Miyazaki, T., Tanaka, H., Kiguchi, T., Fujimoto, K. & Ito, H. 2000 a. Reorientation of  
944 cores and distribution of macroscopic fractures along the GSJ borehole penetrating the  
945 Nojima Fault zone. In: *International workshop of the Nojima Fault core and borehole data*  
946 *analysis* (edited by Ito, H., Fujimoto, K., Tanaka, H. & Lockner, D.) **GSJ Interim report**  
947 **No.EQ/00/1, USGS Open-File Report 000-129**. Geological Survey of Japan, Tsukuba, Japan,  
948 271-276.
- 949 Ohtani, T., Fujimoto, K., Ito, H., Tanaka, H., Tomida, N. & Higuchi, T. 2000 b. Fault rocks and past  
950 to recent fluid characteristics from the borehole survey of the Nojima Fault ruptured in the

- 951 1995 Kobe earthquake, southwest Japan. *Journal of Geophysical Research-Solid Earth*  
952 **105**(B7), 16161-16171.
- 953 Ohtani, T., Tanaka, H., Fujimoto, K., Higuchi, T., Tomida, N. & Ito, H. 2001. Internal structure of  
954 the Nojima Fault zone from the Hirabayashi GSJ drill core. *The Island Arc* **10**(3-4), 392-400.
- 955 Otsuki, K., Monzawa, N. & Nagase, T. 2003. Fluidization and melting of fault gouge during seismic  
956 slip: Identification in the Nojima Fault zone and implications for focal earthquake  
957 mechanisms. *Journal of Geophysical Research-Solid Earth* **108**(B4), 2192,  
958 doi:10.1029/2001JB001711.
- 959 Otsuki, K., Uduki, T., Monzawa, N. & Tanaka, H. 2005. Clayey injection veins and pseudotachylyte  
960 from two boreholes penetrating the Chelungpu Fault, Taiwan: Their implications for the  
961 contrastive seismic slip behaviors during the 1999 Chi-Chi earthquake. *The Island Arc* **14**, 22-  
962 36.
- 963 Otsuki, K., Hirono, T., Ornori, M., Sakaguchi, M., Tanigawa, W., Lin, W. R., Soh, W. & Rong, S. S.  
964 2009. Analyses of pseudotachylyte from Hole-B of Taiwan Chelungpu Fault Drilling Project  
965 (TCDP); their implications for seismic slip behaviors during the 1999 Chi-Chi earthquake.  
966 *Tectonophysics* **469**(1-4), 13-24.
- 967 Pathier, E., Fruneau, B., Deffontaines, B., Angelier, J., Chang, C. P., Yu, S. B. & Lee, C. T. 2003.  
968 Coseismic displacements of the footwall of the Chelungpu Fault by the 1999 Taiwan, Chi-Chi  
969 earthquake from InSAR and GPS data. *Earth and Planetary Science Letters* **212**, 73-88.
- 970 Pezard, P., Ito, H., Hermitte, D. & Revil, A. 2000. Electrical properties and alteration of  
971 granodiorites from the GSJ Hirabayashi hole, Japan. In: *International workshop of the Nojima*  
972 *Fault core and borehole data analysis* (edited by Ito, H., Fujimoto, K., Tanaka, H. & Lockner, D.)  
973 **GSJ Interim report No.EQ/00/1, USGS Open-File Report 000-129**. Geological Survey of  
974 Japan, Tsukuba, Japan, 255-262.
- 975 Rockwell, T., Sisk, M., Girty, G., Dor, O., Wechsler, N. & Ben-Zion, Y. 2009. Chemical and Physical  
976 Characteristics of Pulverized Tejon Lookout Granite Adjacent to the San Andreas and Garlock  
977 Faults: Implications for Earthquake Physics. *Pure and Applied Geophysics* **166**(10-11), 1725-  
978 1746.
- 979 Sibson, R. H. 1973. Interactions between Temperature and Pore-Fluid Pressure During  
980 Earthquake Faulting and a Mechanism for Partial or Total Stress Relief. *Nature-Physical*  
981 *Science* **243**(126), 66-68.
- 982 Sibson, R. H. 1975. Generation of Pseudotachylyte by Ancient Seismic Faulting. *Geophysical*  
983 *Journal of the Royal Astronomical Society* **43**(3), 775-794.
- 984 Sibson, R. H., Moore, J. M. & Rankin, A. H. 1975. Seismic pumping—a hydrothermal fluid  
985 transport mechanism. *Journal of the Geological Society, London* **131**, 653-659.
- 986 Sibson, R. H. 1977. Fault rocks and fault mechanisms. *Journal of the Geological Society of London*  
987 **133**, 191-213.
- 988 Sibson, R. H., Robert, F. & Poulsen, K. H. 1988. High-Angle Reverse Faults, Fluid-Pressure Cycling,  
989 and Mesothermal Gold-Quartz Deposits. *Geology* **16**(6), 551-555.
- 990 Sibson, R. H. 1990. Rupture Nucleation on Unfavorably Oriented Faults. *Bulletin of the*  
991 *Seismological Society of America* **80**(6), 1580-1604.

- 992 Sibson, R. H. 1994. Crustal stress, faulting and fluid flow. In: *Geofluids: origin, migration and*  
993 *evolution of fluids in sedimentary basins* (edited by Parnell, J.) **78**. Geological Society, London,  
994 Special Publications, 69-84, doi:10.1144/GSL.SP.1994.078.01.07.
- 995 Sibson, R. H. 2003. Thickness of the seismic slip zone. *Bulletin of the Seismological Society of*  
996 *America* **93**(3), 1169-1178.
- 997 Sibson, R. H. & Toy, V. G. 2006. The habitat of fault-generated pseudotachylyte: Presence vs.  
998 absence of friction-melt. In: *Earthquakes: Radiated Energy and the Physics of Faulting.*  
999 *Geophysical Monograph Series* **170**, 153-166.
- 1000 Sone, H., Yeh, E. C., Nakaya, T., Hung, J. H., Ma, K. F., Wang, C. Y., Song, S. R. & Shimamoto, T. 2007.  
1001 Mesoscopic structural observations of cores from the Chelungpu Fault system, Taiwan  
1002 Chelungpu-Fault Drilling Project hole-A, Taiwan. *Terrestrial, Atmospheric and Oceanic*  
1003 *Sciences* **18**(2), 359-377.
- 1004 Sone & Shimamoto, T. 2009. Frictional resistance of faults during accelerating and decelerating  
1005 earthquake slip. *Nature Geoscience* **2**, 705-708, DOI: 10.1038/NGE0637.
- 1006 Song, S. R., Kuo, L. W., Yeh, E. C., Wang, C. Y., Hung, J. H. & Ma, K. F. 2007. Characteristics of the  
1007 lithology, fault-related rocks and fault zone structures in TCDP Hole-A. *Terrestrial,*  
1008 *Atmospheric and Oceanic Sciences* **18**(2), 243-269.
- 1009 Sulem, J., Lazar, P. & Vardoulakis, I. 2007. Thermo-poro-mechanical properties of clayey gouge  
1010 and application to rapid fault shearing. *International Journal for Numerical and Analytical*  
1011 *Methods in Geomechanics*, **31**, 523-540.
- 1012 Sulem, J. & Famin, V. 2009. Thermal decomposition of carbonates in fault zones: Slip-weakening  
1013 and temperature-limiting effects. *Journal of Geophysical Research-Solid Earth* **114**, B03309,  
1014 doi:10.1029/2006GL027285.
- 1015 Takahashi, Y. 1992. K-Ar ages of the granitic rocks in Awaji Island with an emphasis on timing of  
1016 mylonitization. *Journal of Mineralogy, Petrology and Economic Geology* **87**, 291-299.
- 1017 Takeshita, T. & Yagi, K. 2001. Paleostress orientation from 3-D orientation distribution of  
1018 microcracks in quartz from the Cretaceous granodiorite core samples drilled through the  
1019 Nojima Fault, south-west Japan. *The Island Arc* **10**(3-4), 495-505.
- 1020 Tanaka, H., Fujimoto, K., Ohtani, T. & Ito, H. 2001 a. Structural and chemical characterization of  
1021 shear zones in the freshly activated Nojima Fault, Awaji Island, southwest Japan. *Journal of*  
1022 *Geophysical Research* **106**(B5), 8789-8810.
- 1023 Tanaka, H., Hinoki, S. I., Kosaka, K., Lin, A. M., Takemura, K., Murata, A. & Miyata, T. 2001 b.  
1024 Deformation mechanisms and fluid behavior in a shallow, brittle fault zone during coseismic  
1025 and interseismic periods: Results from drill core penetrating the Nojima Fault, Japan. *The*  
1026 *Island Arc* **10**(3-4), 381-391.
- 1027 Tanaka, H., Wang, C. Y., Chen, W. M., Sakaguchi, A., Ujiie, K., Ito, H. & Ando, M. 2002. Initial science  
1028 report of shallow drilling penetrating into the Chelungpu Fault zone, Taiwan. *Terrestrial*  
1029 *Atmospheric and Oceanic Sciences* **13**(3), 227-251.
- 1030 Tanaka, H., Chen, W. C., Wang, C. Y., Ma, K. F., Urata, N., Mori, J. & Ando, M. 2006. Frictional heat  
1031 from faulting of the 1999 Chi-Chi, Taiwan earthquake. *Geophysical Research Letters* **33**,  
1032 L16316, doi:10.1029/2006GL026673.
- 1033 Tanaka, H., Omura, K., Matsuda, T., Ikeda, R., Kobayashi, K., Murakami, M. & Shimada, K. 2007 a.  
1034 Architectural evolution of the Nojima Fault and identification of the activated slip layer by

- 1035 Kobe earthquake. *Journal of Geophysical Research-Solid Earth* **112**(B7), B07304,  
1036 doi:10.1029/2005JB003977.
- 1037 Tanaka, H., Chen, W. M., Kawabata, K. & Urata, N. 2007 b. Thermal properties across the  
1038 Chelungpu Fault zone and evaluations of positive thermal anomaly on the slip zones: Are  
1039 these residuals of heat from faulting? *Geophysical Research Letters* **34**, L01309,  
1040 doi:10.1029/2006GL028153.
- 1041 Tanikawa, W. & Shimamoto, T. 2009. Frictional and transport properties of the Chelungpu fault  
1042 from shallow borehole data and their correlation with seismic behavior during the 1999 Chi-  
1043 Chi earthquake. *Journal of Geophysical Research-Solid Earth* **114**, B01402,  
1044 doi:10.1029/2008JB005750.
- 1045 Tanikawa, W., Sakaguchi, M., Hirano, T., Lin, W., Soh, W. & Song, S. R. 2009. Transport properties  
1046 and dynamic processes in a fault zone from samples recovered from TCDP Hole B of the  
1047 Taiwan Chelungpu Fault Drilling Project. *Geochemistry Geophysics Geosystems* **10**(4), Q04013,  
1048 doi:10.1029/2008GC002269.
- 1049 Uehara, S. & Shimamoto, T. 2004. Gas permeability evolution of cataclasite and fault gouge in  
1050 triaxial compression and implications for changes in fault-zone permeability structure  
1051 through the earthquake cycle. *Tectonophysics* **378**(3-4), 183-195.
- 1052 Ujiie, K. 2005. Fault rock analysis of the northern part of the Chelungpu Fault and its relation to  
1053 earthquake faulting of the 1999 Chi-Chi earthquake, Taiwan. *The Island Arc* **14**, 2-11.
- 1054 Wang, J. H., Hung, J. H. & Dong, J. J. 2009. Seismic velocities, density, porosity, and permeability  
1055 measured at a deep hole penetrating the Chelungpu Fault in central Taiwan. *Journal of Asian  
1056 Earth Sciences* **36**(2-3), 135-145.
- 1057 Wibberley, C. A. J. & Shimamoto, T. 2003. Internal structure and permeability of major strike-slip  
1058 fault-zones: the Median Tectonic Line in Mie prefecture, Southwest Japan. *Journal of  
1059 Structural Geology* **25**, 59-78.
- 1060 Wibberley, C. A. J. & Shimamoto, T. 2005. Earthquake slip weakening and asperities explained by  
1061 thermal pressurization. *Nature* **436**, 689-692, doi:10.1038/nature03901.
- 1062 Yamamoto, Y., Kurita, H. & Matsubara, T. 2000. Eocene calcareous nannofossils and  
1063 dinoflagellate cysts from the Iwaya Formation in Awajishima Island, Hyogo Prefecture,  
1064 southwest Japan, and their geologic implications. *Journal of the Geological Society of Japan*  
1065 **106**(5), 379-382.
- 1066 Yeh, E. C., Sone, H., Nakaya, T., Ian, K. H., Song, S. R., Hung, J. H., Lin, W., Hirano, T., Wang, C. Y., Ma,  
1067 K. F., Soh, W. & Kinoshita, M. 2007. Core description and characteristics of fault zones from  
1068 Hole-A of the Taiwan Chelungpu-Fault Drilling Project. *Terrestrial, Atmospheric and Oceanic  
1069 Sciences* **18**(2), 327-357.
- 1070 Yu, S. B., Hsu, Y. J., Kuo, L. C., Chen, H. Y. & Liu, C. C. 2003. GPS measurement of postseismic  
1071 deformation following the 1999 Chi-Chi, Taiwan, earthquake. *Journal of Geophysical Research*  
1072 **108**, 2520, doi: 10.1029/2003JB002396.
- 1073 Yue, L. F., Suppe, J. & Hung, J. H. 2005. Structural geology of a classic thrust belt earthquake: The  
1074 1999 Chi-Chi earthquake Taiwan (Mw7.6). *Journal of Structural Geology* **27**, 2058-2083, doi:  
1075 10.1016/j.jsg.2005.05.020.
- 1076 Zen, E. & Thompson, A. B. 1974. Low grade regional metamorphism: Mineral equilibrium  
1077 relations. *Annual Review of Earth and Planetary Sciences* **2**, 197-212.

1078 Zoback, M. D., Hickman, S. & Ellsworth, W. E. 2007. The role of fault zone drilling. In: *Treatise on*  
1079 *Geophysics* (edited by Schubert, G.) **4**. Elsevier, 649-674.

1080

**Table 1**

Table 1 - Principal occurrences and features of the hydrothermal minerals in the GSJ drill hole (modified from Boullier *et al.* 2004 a).

**Figure captions**

Fig. 1 - (a) Geological map of the northern part of the Awaji Island and location of the DPRI, Hirabayashi GSJ and NIED drill sites [after *Ohtani et al.* 2000 a]. (b) Cross-section showing the vertical offset of the Nojima Fault and the orientation of the DRPI 500 and DPRI 1800 boreholes at Ogura (after *Lin et al.* 2007). (c) Cross-section showing the orientation of the GSJ and NIED boreholes at Hirabayashi (after *Tanaka et al.* 2007 a).

Fig. 2 - Photographs of polished drill core slabs from the Hirabayashi GSJ borehole. The depths of the upper and lower limits of the samples are specified at the top of each image (top of the core always to the left). The sample number (bottom) indicates the number of the drill core box and the number of the sample within that box. The scale marker is 2.5 cm long. (a) Undeformed and almost unaltered Ryoke granodiorite. (b) Very fine-grained compacted ultracataclasite in the core of the fault. Note the reddish colour related to siderite veinlets and the pale honey-coloured veins filled by siderite+ankerite. (c) Very fine-grained compacted ultracataclasite (bottom left) associated with layered pseudotachylytes in the core of the fault.

Fig.3 - Microphotographs of thin sections from the Hirabayashi GSJ borehole. (a) Pseudotachylyte from the sample 99-05 (Fig. 2c, upper right corner). Note the flow structures in the dark brown layer. Plane polarized light. (b) Transparent pseudotachylyte fragment in the ultracataclasite from sample 99-05 (Fig. 2c, lower left corner) which contains numerous CO<sub>2</sub>-rich fluid inclusions (FI). Plane polarized light. (c) Scan of a thin section in sample 100-35 at 633.07m depth showing a clay-rich, low-angle reverse shear zone deforming the fine-grained carbonate veins (short thick arrows). (d) Detail of the shear zone in Fig. 3c showing the C/S arrangement of clays (presumably illite). Crossed polars.

Fig.4 - (a) Sketch of the western Taiwanese foothills showing the principal thrust faults,



the Chi-Chi earthquake epicenter and the location of TCDP drill site. (b) Schematic cross-section passing through the TCDP drill site indicating the principal sedimentary formations and the principal faults (after Hung *et al.* 2007). (c) Correlation between the principal fault zones of the Chelungpu Fault system in Hole A and B (after Hirono *et al.* 2007).

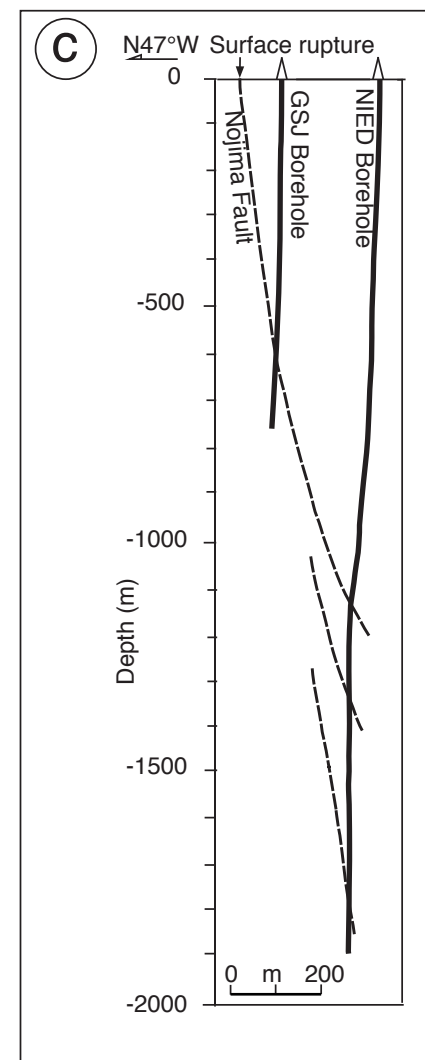
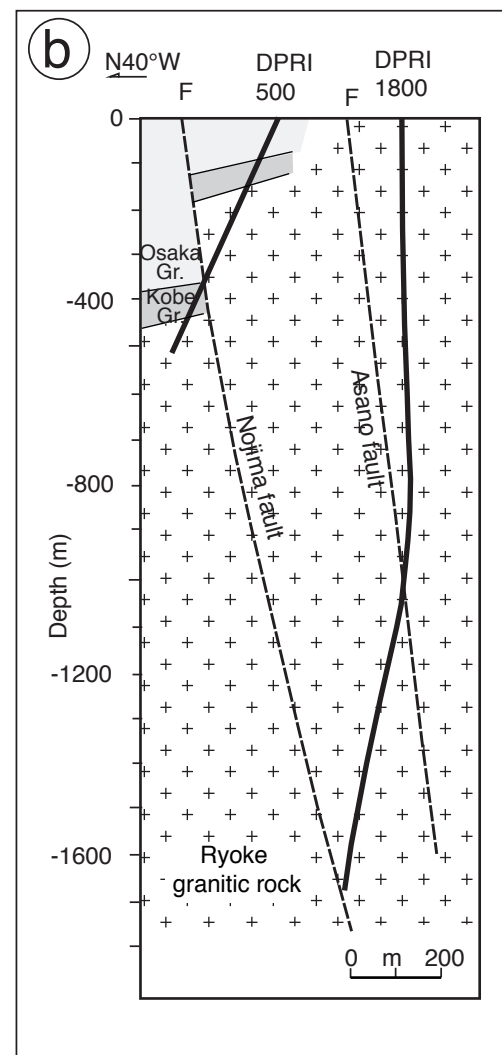
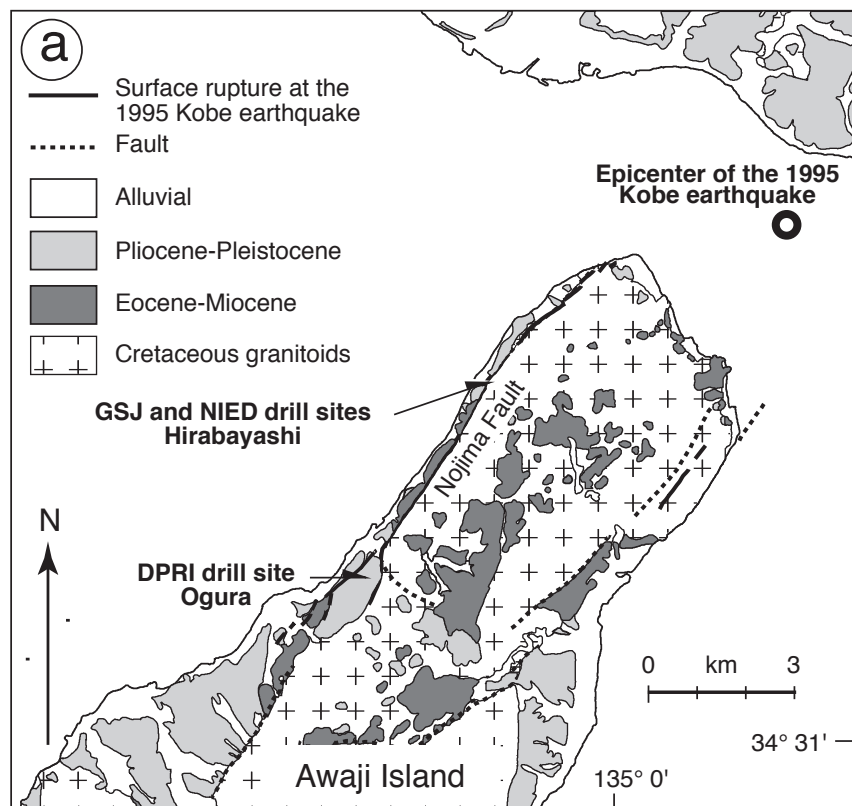
Fig.5 - Sketch (a) and unrolled scanning image (b) of the fault zone of FZA1111 showing the principal structural characteristics of the fault zone activated during the Chi-Chi earthquake. PSZ: Principal Slip Zone (Sibson, 2003) where slip occurred during the Chi-Chi earthquake (after Boullier *et al.* 2009).

Fig. 6 - Microstructures in the isotropic gouge within the PSZ shown in Fig. 5 (after Boullier *et al.* 2009). All microphotographs are oriented as in Fig. 5. (a) General view of the isotropic gouge showing the matrix-supported clasts which are either monomineralic, such as fractured quartz fragment (Q), or fine-grained polymineralic gouge fragments (G). Plane polarized light. (b) Clay-clast aggregate (CCA) with a round quartz core and a brownish cortex made of clays. Plane polarized light.

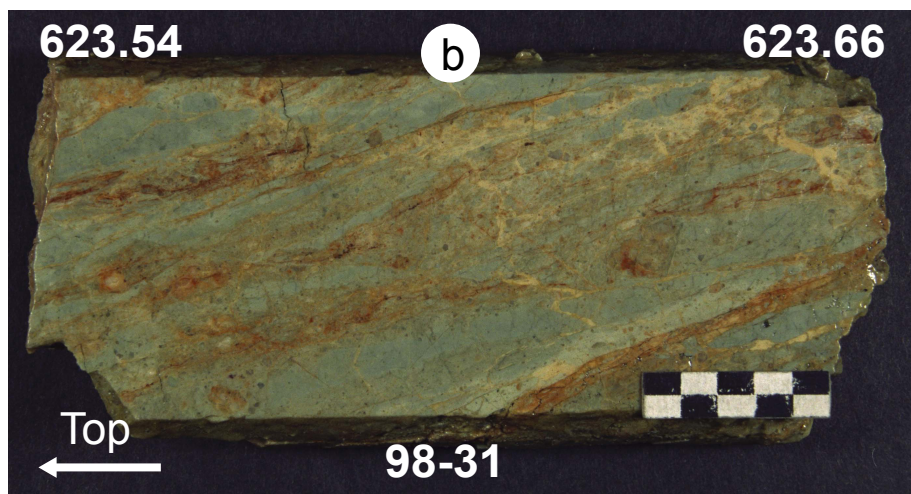
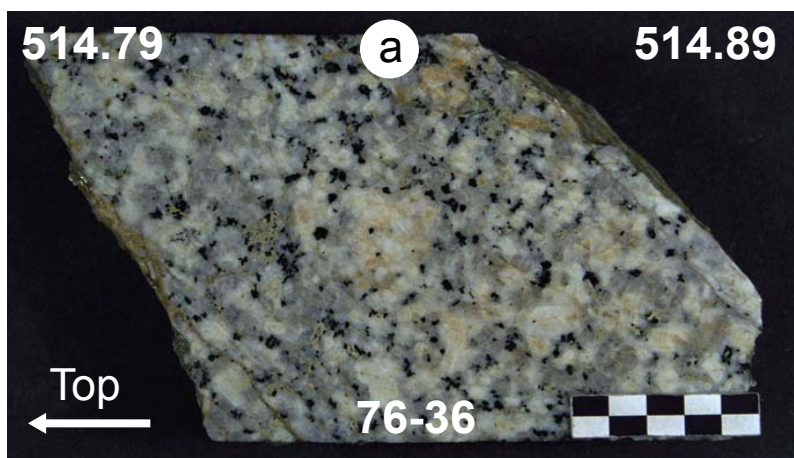
Table 1 - *Hydrothermal episodes in the Nojima Fault*

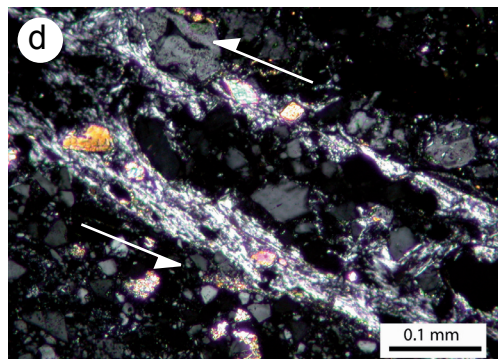
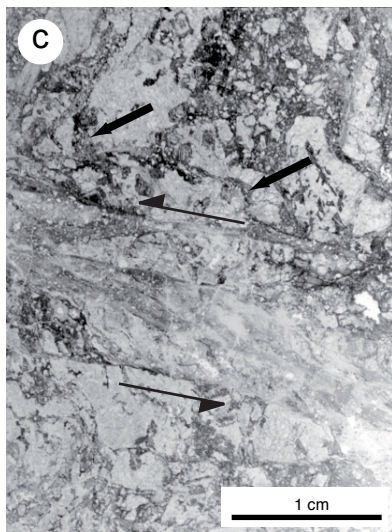
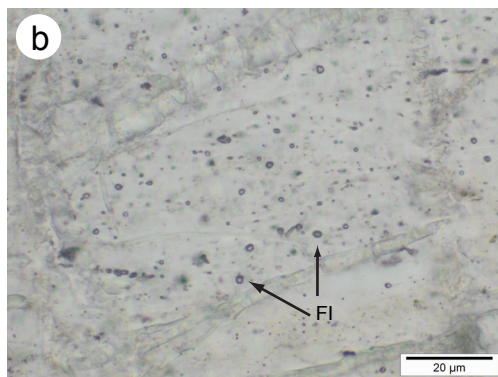
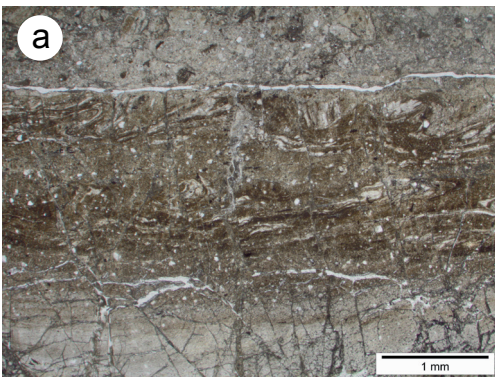
<b>Mineral</b>	<b>Chlorite</b>	<b>Zeolite: laumontite</b> <b>Minor calcite</b>	<b>Siderite</b>	<b>Ankerite and siderite</b>	<b>Clays</b>
Temperature	ca. 300°C	ca. 150-280°C		< 100°C	
Texture	As rosettes in small cavities (ripidolite) In cracks together with albite	In blocky coarse-grained veins In hydraulic fractures, with small fragments of cataclasites or minerals	In thin veinlets parallel to the flattening plane within the core of the fault zone	In hydraulic fractures including fragments of cataclasite and minerals, located above the slip zone	Alteration and replacement of minerals, in fractures, Very fine grained crystals
Replaced mineral	Biotite and amphibole	Plagioclase		Plagioclase, biotite and amphibole	Plagioclase, micas, laumontite
Mechanisms of formation	Hydrothermal processes during cooling of the granodiorite	In-situ replacement Vein filling Hydraulic fracture-fill	Taber growth	Hydraulic fracture-fill	In-situ replacement
Subsequent deformation		Cataclasis Dissolution-precipitation processes: stylolites and veins	Cataclasis	Dissolution-precipitation processes: stylolites and schistosity Cataclasis in thin fine-grained gouge zones	Cataclasis in thin fine-grained gouge and shear zones Orientated parallel to schistosity
Age	Prior to the Kobe Group deposition Between 90 and 74 Ma (*)	Contemporaneous with pseudotachylytes Prior to the Kobe Group deposition ca. 56 Ma (†)	Quiescence stage: between 56 and 1.2 Ma	Younger than ca.1.2 Ma (‡)	Contemporaneous with or younger than carbonates (§)

(\*) After Takahashi (1992) and Murakami and Tagami (2002) - (†) After Murakami and Tagami (2004) - (‡) After Murata et al. (2001) - (§) After Lin et al. (2007).



Boullier Figure 1





Boullier Figure 3

